CHEMISTRY OF MATERIALS

pubs.acs.org/cm

Article

Double Doping of a Low-Ionization-Energy Polythiophene with a Molybdenum Dithiolene Complex

Emmy Järsvall, Till Biskup, Yadong Zhang, Renee Kroon, Stephen Barlow, Seth R. Marder, and Christian Müller*

Cite This: *Chem. Mater.* 2022, 34, 5673−5679

Read Online

ACCESS | Metrics & More | Article Recommendations | Supporting Information

ABSTRACT: Doping of organic semiconductors is crucial for tuning the charge-carrier density of conjugated polymers. The exchange of more than one electron between a monomeric dopant and an organic semiconductor allows the polaron density to be increased relative to the number of counterions that are introduced into the host matrix. Here, a molybdenum dithiolene complex with a high electron affinity of 5.5 eV is shown to accept two electrons from a polythiophene that has a low ionization energy of 4.7 eV. Double p-doping is consistent with the ability of the monoanion salt of the molybdenum dithiolene complex to dope the polymer. The transfer of two electrons to the neutral dopant was also confirmed by electron paramagnetic resonance spectroscopy since the monoanion, but not the dianion, of the molybdenum dithiolene complex features an unpaired electron. Double doping allowed an ionization efficiency of 200% to be reached, which facilitates the design of strongly doped semiconductors while lessening any counterion-induced disruption of the nanostructure.

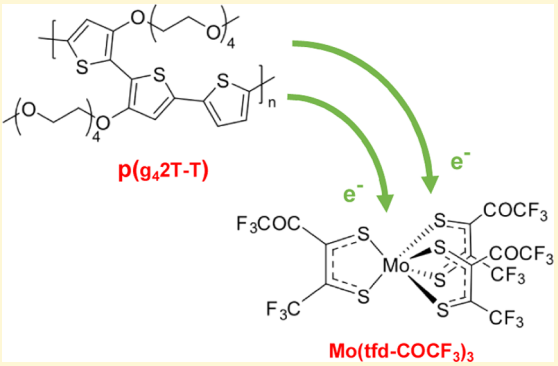

INTRODUCTION

Organic semiconductors attract a great deal of attention since they enable the development of lightweight, flexible, and biocompatible electronic devices for applications from energy harvesting and storage to bioelectronics, which cannot be achieved with inorganic semiconductors alone.[1,2] Doping is a widely used tool to tune the charge-carrier density, which allows the electrical properties of organic semiconductors to be optimized.[3−5] The process typically involves the addition of a dopant, such as an organic molecule, a metal−organic complex, or a metallic salt, that undergoes an electron transfer with the organic semiconductor.[5] Electron transfer readily occurs in the case of a favorable energetic offset between the two materials. In the case of p-doping, for example, it is beneficial if the dopant has an electron affinity (EA) that is larger than the ionization energy (IE) of the semiconductor, i.e., $EA_{dopant} \geq IE_{semiconductor}$. Here, it is important to note that the EA and IE, which are often estimated from electrochemical methods, can take on very different values once the dopant and semiconductor are mixed.[6] Furthermore, the structural and energetic disorder inherent to many organic semiconductors leads to a broad density of states, which may facilitate some degree of electron transfer despite an unfavorable energy offset.[7,8] Provided that each p-dopant accepts one electron from the semiconductor, i.e., the pair undergoes integer charge transfer, one polaron is created per dopant molecule, resulting in an ionization efficiency of 100%. The ionization efficiency is reduced to less than 100% in the case that only partial charge transfer occurs, if there is an unfavorable energetic offset between EA_{dopant} and $IE_{semiconductor}$ or if the dopant molecules aggregate. The presence of excess dopants and dopant aggregates unduly disrupts the nanostructure of the semiconductor, which tends to negatively affect the electrical properties.[9−11]

We have recently reported that quinodimethane-type dopants with a sufficiently high EA_{dopant} can accept two electrons from a low-IE conjugated polymer, resulting in an ionization efficiency of 200%.[12] This type of double doping was observed for a thienothiophene-based copolymer with tetraethylene glycol side chains, for which $IE_{polymer}$ = 4.5 eV, doped with either 2,3,5,6-tetrafluoro-7,7,8,8-tetracyanoquinodimethane (F_4TCNQ), for which EA_{F_4TCNQ} = 5.2 eV, or 1,3,4,5,7,8-hexafluorotetracyanonaphthoquinodimethane (F_6TCNNQ), for which EA_{F_6TCNNQ} = 5.3 eV (electron affinity estimated from half-wave potential $E_{1/2}$ vs ferrocene/ferrocenium, Fc/Fc^+; EA_{dopant} = 5.1 eV + $E_{1/2}$).[12] The electron

Received: April 6, 2022
Revised: May 25, 2022
Published: June 13, 2022

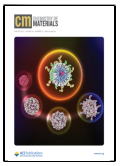

https://doi.org/10.1021/acs.chemmater.2c01040
Chem. Mater. 2022, 34, 5673−5679

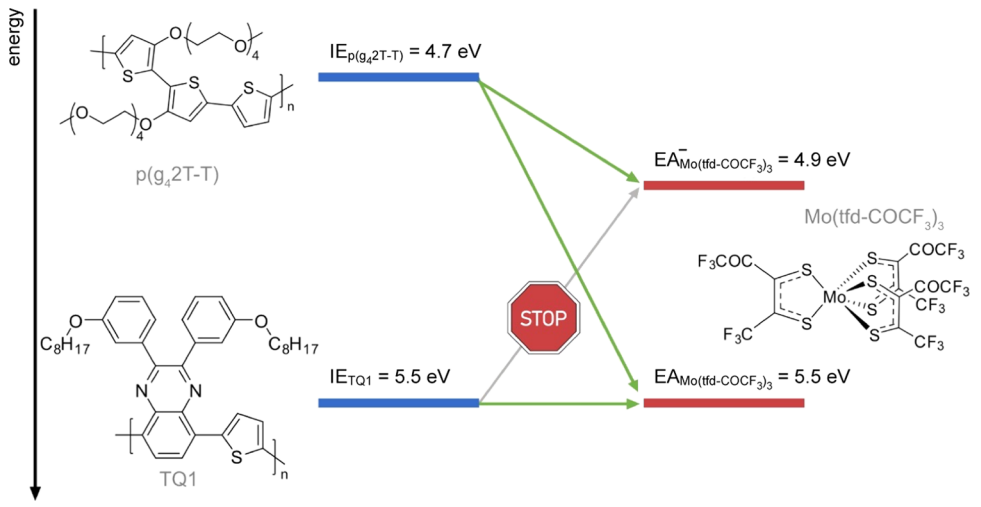

Figure 1. Energy diagram showing the energy levels that are relevant for charge transfer from polymers p($g_4$2T-T) and TQ1 to the p-type dopant Mo(tfd-$COCF_3$)$_3$.

affinities of the anions of these two quinodimethane-type dopants, EA^-_{dopant}, are estimated to remain sufficiently low that $EA^-_{dopant} > IE_{polymer}$, allowing each dopant to accept a second electron from the polymer. Other dopants that can give rise to more than one polaron include the dimers formed by certain 19-electron organometallic sandwich compounds or by benzoimidazoline radicals, the overall reaction of which with a host results in the formation of two monomeric dopants and the release of two electrons.[7] These dopant dimers, however, have approximately twice the molecular volume of related monomeric dopants, which reduces the benefit of double doping because it doubles the overall volume that is occupied by counterions. Likewise, multivalent radical cation salts that comprise two or four triphenylamine units can accept two or even four electrons from a conjugated polymer[13,14] but have a close to 2−4 times larger volume compared to the corresponding monovalent radical anion salt tris(4-bromophenyl)ammoniumyl hexachloroantimonate ([TPA−Br_3]$^+$[$SbCl_6$]$^-$; Magic Blue). We argue that double doping is preferably achieved without increasing the size of the dopant so that fewer dopant molecules must be added to obtain a certain polaron density, which reduces the risk of dopant aggregation and lessens the impact of doping on the nanostructure of the polymer.

Here we ask whether double doping is unique to quinodimethane-type monomeric dopants or whether it is a generic concept that can also be observed for other species. In particular, we investigate doping using the dithiolene complex Mo(tfd-$COCF_3$)$_3$,[15] for which $EA_{Mo(tfd\text{-}COCF_3)_3}$ can be estimated as ca. 5.5 eV (reduction potential $E_{red} \approx +0.39$ V vs decamethylferrocene/decamethylferrocenium, DmFc/DmFc$^+$; $EA_{Mo(tfd\text{-}COCF_3)_3} = 5.1$ eV + E_{red}).[16] We note that electrochemically based estimates of the electron affinity are approximate because solvation effects and solid-state polarization effects likely vary between molecules of different sizes and shapes. However, the value of $EA_{Mo(tfd\text{-}COCF_3)_3} = 5.5$ eV is in reasonable agreement with a value of 5.6 eV measured in the solid state by inverse photoelectron spectroscopy for a related molecule, Mo(tfd)$_3$, for which $E_{red} \approx +0.28$ V vs DmFc/DmFc$^+$.[17] Mo(tfd-$COCF_3$)$_3$ has been used to dope a wide range of conjugated polymers including poly(3-hexylthiophene) (P3HT),[18,19] poly[2,5-bis(3-tetradecylthiophen-2-yl)thieno-[3,2-*b*]thiophene] (PBTTT),[20,21] and a benzodithiophene-based copolymer.[9,22,23] We chose Mo(tfd-$COCF_3$)$_3$ because it can exist both as an anion and dianion, meaning that it can sustain two electron transfer events, and both of these species are known to have reasonable chemical stability (indeed, the neutral dopant is obtained by chemical oxidation of the dianion).[16] The Mo(tfd-$COCF_3$)$_3$ anion electron affinity, $EA^-_{Mo(tfd-COCF_3)_3}$, can be estimated as ca. 4.9 eV ($E_{red} \approx -0.16$ V vs Fc/Fc$^+$),[16] although the potential separation between subsequent redox processes in electrochemical experiments can be highly medium-dependent,[24] meaning there will be a larger uncertainty in this estimate than in those of the electron affinity of neutral molecules. Nevertheless, if $EA^-_{Mo(tfd-COCF_3)_3}$ is indeed ca. 4.9 eV, then polymers with an $IE_{polymer} < 4.9$ eV should be able to experience double doping when brought in contact with Mo(tfd-$COCF_3$)$_3$. Doping of two polymers was investigated, the polythiophene p($g_4$2T-T) with tetraethylene glycol side chains and a low $IE_{p(g_4 2T-T)} = 4.7$ eV (oxidation potential $E_{ox} \approx -0.44$ V vs Fc/Fc$^+$; $IE_{p(g_4 2T-T)} = 5.1$ eV + E_{ox})[25] and the thiophene-quinoxaline copolymer TQ1,[26,27] which features a large $IE_{TQ1} = 5.5$ eV ($E_{ox} \approx 0.37$ V vs Fc/Fc$^+$;[27] see Figure 1 for chemical structures and energy levels). We here show that p($g_4$2T-T) readily undergoes double doping by Mo(tfd-$COCF_3$)$_3$.

RESULTS AND DISCUSSION

The dopant investigated here can exist as a neutral complex, Mo(tfd-$COCF_3$)$_3$, as well as a salt comprising either its anion or dianion. The dianion salt Mo(tfd-$COCF_3$)$_3$(Et_4N)$_2$ is a precursor for the synthesis of Mo(tfd-$COCF_3$)$_3$, as reported previously.[15,16] Neutral Mo(tfd-$COCF_3$)$_3$ was prepared by oxidizing the dianion salt using $NOPF_6$. The anion salt, instead, was prepared by the comproportionation of equimolar amounts of Mo(tfd-$COCF_3$)$_3$ and the dianion salt Mo(tfd-$COCF_3$)$_3$ (Et_4N)$_2$. All three species give rise to distinct ultraviolet−visible−near-infrared (UV−vis−NIR) absorbance spectra (Figure 2a). These absorptions, however, occur at wavelengths where either neat p($g_4$2T-T) and TQ1 absorb or where polaronic absorbance peaks tend to arise upon doping. Hence, it is challenging to extract information about the

https://doi.org/10.1021/acs.chemmater.2c01040
Chem. Mater. 2022, 34, 5673−5679

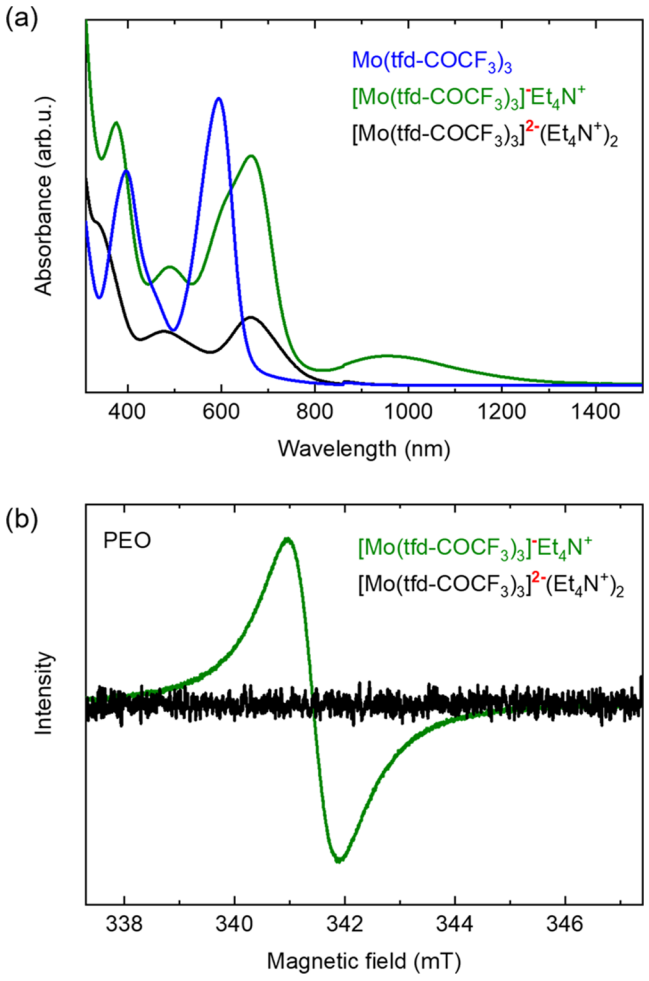

Figure 2. (a) UV−vis spectra of $Mo(tfd\text{-}COCF_3)_3$, $[Mo(tfd\text{-}COCF_3)_3]^-Et_4N^+$, and $[Mo(tfd\text{-}COCF_3)_3]^{2-}(Et_4N^+)_2$ dissolved in dichloromethane (DCM). (b) EPR spectra of $[Mo(tfd\text{-}COCF_3)_3]^-Et_4N^+$ and $[Mo(tfd\text{-}COCF_3)_3]^{2-}(Et_4N^+)_2$ dispersed in a matrix of poly(ethylene oxide) (PEO; see Figure S4 for nonsmoothed EPR spectra).

presence of different species from optical spectroscopy. Instead, we chose to use electron paramagnetic resonance (EPR) spectroscopy to detect the presence of different species.

In a first set of experiments, we recorded EPR spectra of the monoanion salt and the dianion salt dispersed in poly(ethylene oxide) (PEO) to mimic the solid-state environment that the two species will experience when dispersed in a p($g_4$2T-T) matrix. The UV−vis−NIR spectra of the monoanion and dianion salt dissolved in dichloromethane (DCM) or in PEO are comparable (Figure S1), which suggests that the PEO matrix does not strongly alter the electronic state of the two species. The monoanion salt gives rise to a distinct EPR signal centered at B_0 = 341.4 mT, in agreement with reports for other monoanionic molybdenum tris(dithiolene) complexes,[28−30] while the dianion salt appears spin-silent (Figures 2b and S2−S4), consistent with the sharp NMR spectra reported for $[Mo(tfd\text{-}COCF_3)_3]^{2-}$,[15] as well as with magnetic susceptibility[30] and computational studies[31] of other molybdenum tris(dithiolene) dianions.

We next studied doped TQ1, which has a high IE_{TQ1} = 5.5 eV that is comparable to $EA_{Mo(tfd\text{-}COCF_3)_3}$. Judging by the ionization energy of TQ1, the polymer can be expected to undergo some electron transfer with neutral $Mo(tfd\text{-}COCF_3)_3$, but the energy levels of TQ1 and $[Mo(tfd\text{-}COCF_3)_3]^-$ should not allow for a second charge transfer event since $IE_{TQ1} \gg EA^-_{Mo(tfd-COCF_3)_3}$. UV−vis−NIR spectra of TQ1 sequentially doped with $Mo(tfd\text{-}COCF_3)_3$ reveal clear polaronic absorption bands confirming that electron transfer has indeed occurred (Figure 3a). The EPR spectra for TQ1 doped with $Mo(tfd\text{-}COCF_3)_3$ consist of two overlapping signals, one at a magnetic field of 342.2 mT and one at a lower magnetic field. We assign the signal at a lower magnetic field to the monoanion of $Mo(tfd\text{-}COCF_3)_3$ since it appears at the same position as the EPR signal observed for $[Mo(tfd\text{-}COCF_3)_3]^-Et_4N^+$ (Figures 3b, S5, and S6). This observation suggests that doping of TQ1 with $Mo(tfd\text{-}COCF_3)_3$ primarily occurs through a single electron transfer event per dopant, resulting in $Mo(tfd\text{-}COCF_3)_3$ anions that can be detected with EPR spectroscopy.

To confirm the plausibility of assigning the EPR signal at 342.2 mT to the polymer polaron, we also recorded EPR spectra of TQ1 doped with Magic Blue, which is a stronger oxidant than $Mo(tfd\text{-}COCF_3)_3$ and in which the radical cation portion can accept an electron from TQ1 because neutral tris(4-bromophenyl)amine (TPA−Br_3) has a very high $IE_{TPA-Br_3} \approx 5.7$ eV ($E_{1/2}$ = +0.7 V vs DmFc/DmFc$^+$),[32] i.e., its radical cation $[TPA-Br_3]^+$ can be reduced by TQ1 since 5.7 eV > IE_{TQ1}. Doping of TQ1 with Magic Blue is confirmed by the appearance of a strong polaron absorption band at 900 nm in recorded UV−vis spectra (Figure 3a).[33] The tris(4-bromophenyl)ammoniumyl cation $[TPA-Br_3]^+$ becomes neutral as it receives an electron from the polymer during the doping process, and hence ends up spin-silent. Consequently, the EPR spectrum of doped TQ1 exclusively features a polaron signal. The similarity of the signal at ca. 342.2 mT seen for $Mo(tfd\text{-}COCF_3)_3$-doped TQ1 to the EPR spectrum of TQ1 doped with Magic Blue confirms that this signal arises from polarons on TQ1 (Figures 3c, S7, and S8).

In a further set of experiments, we studied sequential doping of p($g_4$2T-T) with neutral $Mo(tfd\text{-}COCF_3)_3$ as well as its anion salt, i.e., the two species were allowed to ingress from a dopant solution into a solid film of the polymer (see the Experimental Section for details). UV−vis−NIR spectroscopy reveals stronger polaron absorption bands at 900 nm and in the near-infrared region for p($g_4$2T-T) doped with the neutral complex, which indicates a higher degree of doping with $Mo(tfd\text{-}COCF_3)_3$ compared to doping with the monoanion salt (Figure 4a). Moreover, the fact that we can dope p($g_4$2T-T) with the monoanion suggests that double doping is possible for this system. Doping of p($g_4$2T-T) with $Mo(tfd\text{-}COCF_3)_3$ gives rise to an electrical conductivity of σ = (19.6 ± 0.6) S cm^{-1}, whereas doping with the monoanion salt gives a value of σ = (11.9 ± 0.3) S cm^{-1}. The higher electrical conductivity for p($g_4$2T-T) doped with the neutral complex is also an indication that we have a higher degree of doping, i.e., a larger number of charge carriers in this sample compared to p($g_4$2T-T) doped with the monoanion salt. EPR spectra of neat p($g_4$2T-T) as well as the polymer doped with either neutral $Mo(tfd\text{-}COCF_3)_3$ or the anion salt all reveal a polaron signal at g = 342.2 mT (Figures 4b and S9). The signal in the case of the neat p($g_4$2T-T) sample likely arises from adventitious oxygen doping of the polymer. In the case of doping with the neutral complex, the recorded EPR spectrum features a broad shoulder at a lower magnetic field around 341 mT, which we explain with the presence of monoanions, i.e.,

https://doi.org/10.1021/acs.chemmater.2c01040
Chem. Mater. 2022, 34, 5673−5679

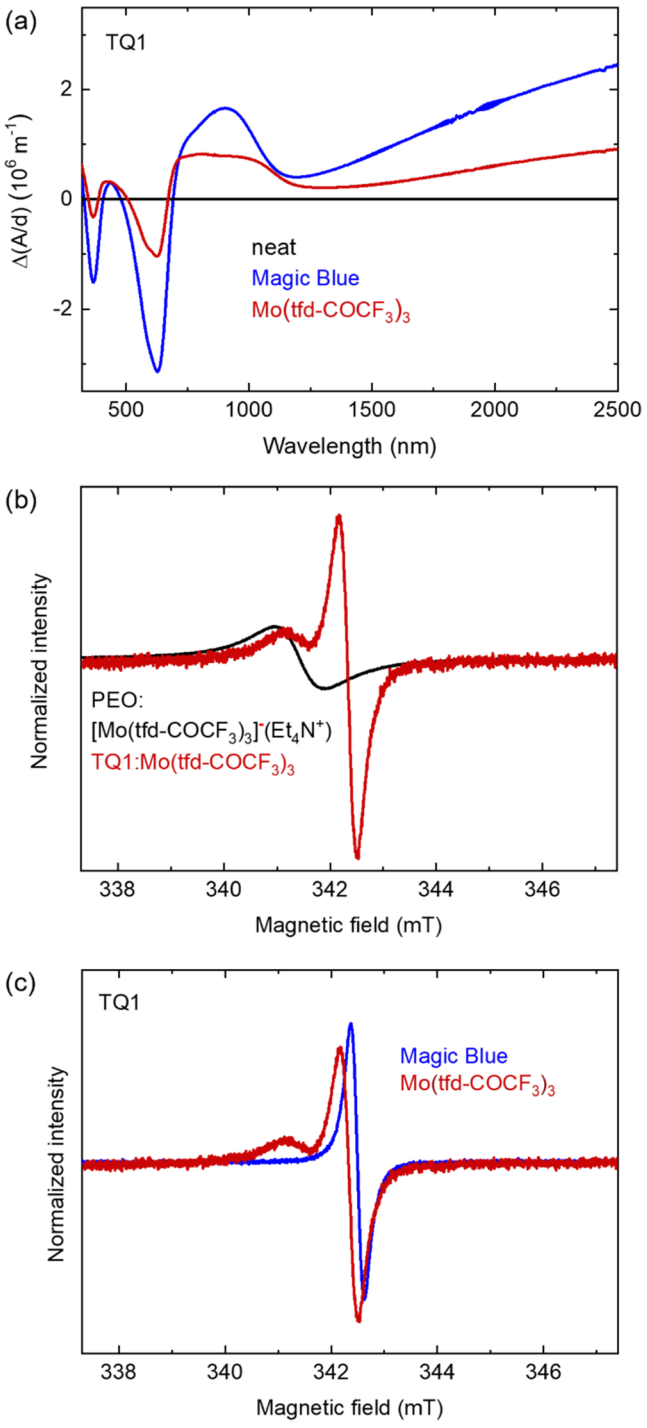

Figure 3. (a) UV−vis−NIR absorbance spectra displaying the difference in thickness-normalized absorbance $\Delta(A/d)$ between the spectra of neat TQ1 and TQ1 doped with Magic Blue or Mo(tfd-$COCF_3)_3$. (b) EPR spectra of $[Mo(tfd\text{-}COCF_3)_3]^-Et_4N^+$ dispersed in a PEO matrix and TQ1 doped with Mo(tfd-$COCF_3)_3$. The spectra have been normalized to the maximum in the field range 338−341.5 mT. (c) EPR spectra of TQ1 doped with Magic Blue or Mo(tfd-$COCF_3)_3$. The spectra have been normalized to the same amplitude.

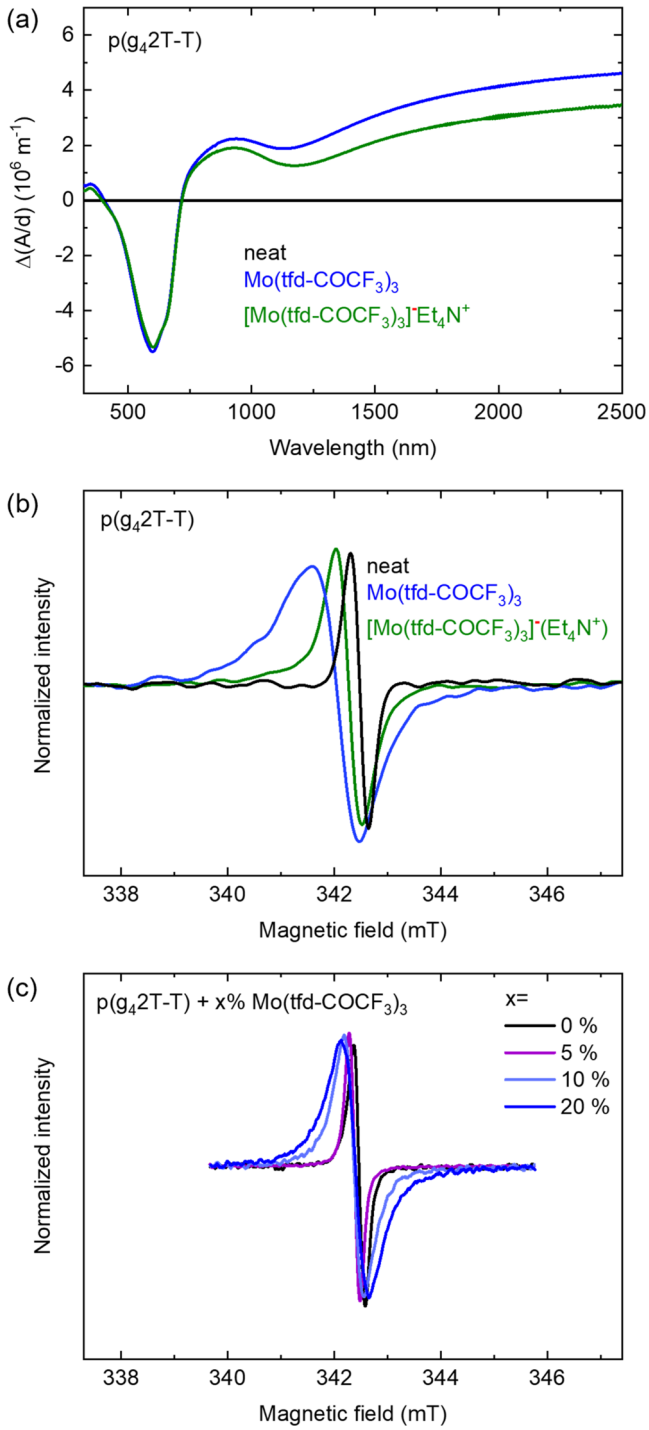

Figure 4. (a) UV−vis−NIR absorbance spectra displaying the difference in thickness-normalized absorbance $\Delta(A/d)$ between the spectra of neat p($g_4$2T-T) and p($g_4$2T-T) sequentially doped with Mo(tfd-$COCF_3)_3$ or $[Mo(tfd\text{-}COCF_3)_3]^-Et_4N^+$. (b) EPR spectra of neat p($g_4$2T-T) and p($g_4$2T-T) sequentially doped with Mo(tfd-$COCF_3)_3$ or $[Mo(tfd\text{-}COCF_3)_3]^-Et_4N^+$. (c) EPR spectra of co-processed p($g_4$2T-T):Mo(tfd-$COCF_3)_3$ films (see Figures S9 and S11 for nonsmoothed EPR spectra).

the EPR spectrum is a superposition of the EPR signal of the polaron on the polymer and the EPR signal of the monoanion. The EPR spectrum of p($g_4$2T-T) sequentially doped with the monoanion features a signal at a similar field as the neat, oxygen-doped polymer, and the absence of a broad shoulder around 341 mT suggests that no major fraction of monoanions is present. Since UV−vis−NIR spectroscopy indicates that the polymer was doped, i.e., polarons were generated (see Figure 4a), the majority of monoanions that have entered the polymer

https://doi.org/10.1021/acs.chemmater.2c01040
Chem. Mater. 2022, 34, 5673−5679

Table 1. Parameters Quantifying the Extent of Doping and the Resulting Conductivity and Mobility for p(g$_4$2T-T) Co-Processed with Different Amounts of Mo(tfd-COCF$_3$)$_3$; Amount of Dopant in mol %, Calculated Relative to the Molar Mass of the Repeat Unit of p(g$_4$2T-T), Oxidation Level O_{ox}, i.e., Number of Polarons Per Polymer Thiophene Ring in Percent, Ionization Efficiency η_{ion}, i.e., Number of Polarons Per Added Dopant Molecules in Percent, Number of Polarons N_p, Conductivity σ and Mobility $\mu = \sigma e N_p$, where e is the Elementary Charge

mol % dopant	O_{ox} (%)	η_{ion} (%)	N_p (10^{26} m^{-3})	σ (S cm^{-1})	μ (cm^2 V^{-1} s^{-1})
5	3.4 ± 0.2	195 ± 3	0.94 ± 0.02	0.05 ± 0.01	0.003 ± 0.001
10	7.4	200[a]	2.0	1.1 ± 0.1	0.03 ± 0.01
20	13.1 ± 0.2	158 ± 2.3	3.6 ± 0.1	15 ± 1	0.26 ± 0.04

[a]For 10 mol % dopant, the calculated value of η_{ion} was larger than physically possible and therefore was set to 200%.

film must have accepted an electron from p(g$_4$2T-T) and thus became spin-silent dianions.

Finally, we studied a series of p(g$_4$2T-T) thin films that were prepared by co-processing the polymer with different amounts of the neutral Mo-complex. The conductivity increases with the amount of dopant (Table 1) and the polaron absorbance increases (see UV−vis−NIR spectra in Figure S10), which is consistent with an increasing polaron concentration. For all co-processed samples, the EPR signal is centered at 342.2 mT, i.e., the position assigned to polarons, and we do not observe any broad shoulder at lower magnetic fields (Figures 4c and S11). However, we instead observe a symmetrical broadening with increasing dopant concentration. We interpret the lack of the low-field shoulder as an indication that no significant amount of monoanions is present and hence the EPR signal solely originates from the polarons. The observed symmetrical broadening of the EPR signal with increasing dopant concentration could be attributed to a spin−spin interaction between nearby polarons.[34] Another explanation for the observed symmetrical broadening could be a lower degree of interchain charge hopping with increasing dopant concentrations resulting in the transition from Lorentzian to Gaussian absorption features.[35]

We used the UV−vis−NIR spectra of the co-processed samples to estimate the number of polarons N_p (Table 1). To estimate N_p we compared the thickness-normalized difference in absorbance $\Delta(A_{800}/d)$ between doped samples and the neat polymer at 800 nm, where a pronounced sub-bandgap polaronic absorption peak is situated, with the molar attenuation coefficient of the polaronic absorption obtained from electrochemically doped P3HT at 800 nm, $\varepsilon_{800} = (4.1 \pm 0.2) \times 10^3$ m^2 mol^{-1}.[19] The Beer−Lambert law $\Delta(A_{800}/d) = \varepsilon_{800} \times N_p$, where d is the film thickness, was used to estimate N_p. We then calculated the oxidation level according to $O_{ox} = N_p/N_{thiophene}$ and ionization efficiency according to $\eta_{ion} = N_p/N_{Mo(tfd-COCF_3)_3}$, where $N_{Mo(tfd-COCF_3)_3}$ is the number of molybdenum dithiolene complexes (Table 1). We obtain an ionization efficiency of more than 100% for all studied samples, indicating that double doping occurs even for the samples with a higher doping concentration. For 5 and 10 mol % dopants, we estimate that the ionization efficiency is close to 200%, meaning that each Mo(tfd-COCF$_3$)$_3$ complex accepts two electrons from p(g$_4$2T-T). A high degree of double doping explains why we do not observe any clear feature of the monoanion in the EPR spectra of p(g$_4$2T-T) co-processed with Mo(tfd-COCF$_3$)$_3$ (Figure 4c). Most of the monoanions that form undergo a second electron transfer event and thus become dianions, which are spin-silent.

CONCLUSIONS

We conclude that the molybdenum dithiolene complex Mo(tfd-COCF$_3$)$_3$ can accept two electrons from the conjugated polymer p(g$_4$2T-T). The dopant monoanions could be detected with EPR spectroscopy because their signal appears at a lower magnetic field than the signal from the polymer polaron. The absence of a clear monoanion signal in EPR spectra of the polymer co-processed with Mo(tfd-COCF$_3$)$_3$ suggests that only dianions are present, i.e., the dopant underwent two electron transfer events with the polymer. The viability of double doping was confirmed by sequential doping of polymer films with the monoanion salt [Mo(tfd-COCF$_3$)$_3$]$^-$Et$_4$N$^+$, which gave rise to a conductivity of $\sigma = (11.9 \pm 0.3)$ S cm^{-1} and EPR spectra that did not feature any signal from anions, indicating that each anion had been converted into a spin-silent dianion by accepting one electron from the polymer. Analysis of the UV−vis−NIR spectra of co-processed samples indicated an ionization efficiency of 200% for use of up to 10 mol % Mo(tfd-COCF$_3$)$_3$. It can be anticipated that double doping of polymers with suitable monomeric dopants may allow us to achieve high charge-carrier densities while reducing the number of counterions and hence their collective impact on the nanostructure of semiconductor films.

EXPERIMENTAL SECTION

Materials. TQ1 (weight- and number-average molecular weights, M_n = 76 kg mol^{-1} and PDI = 2.6), p(g$_4$2T-T) (M_n = 24 kg mol^{-1}, PDI = 3.3), Mo(tfd-COCF$_3$)$_3$, and [Mo(tfd-COCF$_3$)$_3$]$^-$Et$_4$N$^+$ and [Mo(tfd-COCF$_3$)$_3$]$^{2-}$(Et$_4$N$^+$)$_2$ were prepared according to previously reported procedures.[15,27,36] Poly(ethylene oxide) (PEO, M_w = 200 kg mol^{-1}), [TPA−Br$_3$]$^+$[SbCl$_6$]$^-$ (Magic Blue), dichloromethane (DCM, purity > 99.9%), and anhydrous acetonitrile (AcN, purity > 99.8%) were purchased from Sigma-Aldrich. Chlorobenzene (CB, purity > 99%) and chloroform (CHCl$_3$, purity > 99.8%) were obtained from Fisher Scientific. All commercial solvents and the Magic Blue dopant were used as received and without further purification.

Sample Preparation. Polymers were dissolved with a concentration of 10 g L^{-1} (TQ1 in CB and p(g$_4$2T-T) in CHCl$_3$) and spin-cast onto poly(ethylene terephthalate) (PET) films, yielding a film thickness of 50−100 nm. The polymer films were sequentially doped with Magic Blue dissolved in AcN/CHCl$_3$ (3:1, v/v; 0.45 g L^{-1}), Mo(tfd-COCF$_3$)$_3$ in AcN/CHCl$_3$ (3:1, v/v; 2.5 g L^{-1}), and [Mo(tfd-COCF$_3$)$_3$]$^-$Et$_4$N$^+$ in AcN/DCM (3:2, v/v; 2.5 g L^{-1}). The dopant solutions were added on top of the films for 30 s, spun off, and finally the films were rinsed with anhydrous AcN to remove any excess dopant on top of the film. To prepare co-processed p(g$_4$2T-T)/Mo(tfd-COCF$_3$)$_3$ samples, p(g$_4$2T-T) and Mo(tfd-COCF$_3$)$_3$ were dissolved in AcN/CHCl$_3$ (1:1, v/v; 15 and 5 g L^{-1}). Appropriate volumes of AcN/CHCl$_3$ (1:1, v/v) were then added to the p(g$_4$2T-T) solutions before the addition of the Mo(tfd-COCF$_3$)$_3$ solution to maintain a polymer concentration of 5−7.5 g L^{-1} in each polymer/dopant solution while varying the concentration of Mo(tfd-COCF$_3$)$_3$.

https://doi.org/10.1021/acs.chemmater.2c01040
Chem. Mater. 2022, 34, 5673−5679

The co-processed polymer/dopant solutions were spin-cast onto PET films, yielding a film thickness of 80−200 nm. The calculations of molar percentage were based on the molar mass of the polymer repeat unit and the molar mass of the dopant. $Mo(tfd\text{-}COCF_3)_3$, $[Mo(tfd\text{-}COCF_3)_3]^-Et_4N^+$, and $[Mo(tfd\text{-}COCF_3)_3]^{2-}(Et_4N^+)_2$ were dissolved together with PEO in DCM (4 and 16 g L^{-1}), and the solutions were then spin-cast onto PET films.

UV−vis−NIR Absorption Spectroscopy. Measurements of liquid and solid samples were performed with a PerkinElmer Lambda 1050 spectrometer. $Mo(tfd\text{-}COCF_3)_3$, $[Mo(tfd\text{-}COCF_3)_3]^-Et_4N^+$, and $[Mo(tfd\text{-}COCF_3)_3]^{2-}(Et_4N^+)_2$ solutions for UV−vis−NIR absorption measurements were prepared at a concentration of 1 g L^{-1} in DCM.

Electron Paramagnetic Resonance. The polymer films coated on PET films were cut to a size of 25 mm × 3 mm and then sealed under nitrogen in a quartz EPR tube. EPR spectra were recorded at room temperature using a Magnettech MS5000 spectrometer (Freiberg Instruments, now Bruker Biospin). All spectra were corrected for the same microwave frequency (9.6 GHz). Data processing and analysis have been performed using the cwepr Python package.[37,38]

Electrical Characterization. The electrical resistivity was measured with a four-point probe setup from Jandel Engineering (cylindrical probe head, RM3000) using collinear tungsten carbide electrodes with an equidistant spacing of 1 mm that were held down with a constant weight of 60 g. The electrical conductivity σ was then calculated according to $\sigma = ((V/I)kt)^{-1}$, where V is the voltage, I is the current, $k = 4.53$ is a geometrical correction factor, and t is the thickness.

■ ASSOCIATED CONTENT

Supporting Information

The Supporting Information is available free of charge at https://pubs.acs.org/doi/10.1021/acs.chemmater.2c01040.

UV−vis−NIR spectra as well as angular-dependent and nonsmoothed EPR spectra (PDF)

■ AUTHOR INFORMATION

Corresponding Author

Christian Müller − *Department of Chemistry and Chemical Engineering, Chalmers University of Technology, 41296 Göteborg, Sweden;* orcid.org/0000-0001-7859-7909; Email: christian.muller@chalmers.se

Authors

Emmy Järsvall − *Department of Chemistry and Chemical Engineering, Chalmers University of Technology, 41296 Göteborg, Sweden*

Till Biskup − *Physical Chemistry, University of Saarland, Saarbrücken 66123, Germany;* orcid.org/0000-0003-2913-0004

Yadong Zhang − *Georgia Institute of Technology, School of Chemistry and Biochemistry and Center for Organic Photonics and Electronics, Atlanta, Georgia 30332-0400, United States; Renewable and Sustainable Energy Institute, University of Colorado Boulder, Boulder, Colorado 80303, United States*

Renee Kroon − *Department of Chemistry and Chemical Engineering, Chalmers University of Technology, 41296 Göteborg, Sweden; Laboratory of Organic Electronics, Linköping University, 60174 Norrköping, Sweden;* orcid.org/0000-0001-8053-4288

Stephen Barlow − *Georgia Institute of Technology, School of Chemistry and Biochemistry and Center for Organic Photonics and Electronics, Atlanta, Georgia 30332-0400, United States; Renewable and Sustainable Energy Institute, University of Colorado Boulder, Boulder, Colorado 80303, United States;* orcid.org/0000-0001-9059-9974

Seth R. Marder − *Georgia Institute of Technology, School of Chemistry and Biochemistry and Center for Organic Photonics and Electronics, Atlanta, Georgia 30332-0400, United States; Renewable and Sustainable Energy Institute, University of Colorado Boulder, Boulder, Colorado 80303, United States; Departments of Chemical and Biological Engineering and of Chemistry, University of Colorado Boulder, Boulder, Colorado 80303, United States*

Complete contact information is available at: https://pubs.acs.org/10.1021/acs.chemmater.2c01040

Notes

The authors declare no competing financial interest.

EPR raw data and analysis "recipes" used to analyze the EPR data are available online via Zenodo (DOI: 10.5281/zenodo.6592331).

■ ACKNOWLEDGMENTS

The authors acknowledge funding from the Swedish Research Council through grant agreement no. 2018-03824 and the National Science Foundation through a DMREF award, DMR-1729737.

■ REFERENCES

(1) *Organic Flexible Electronics: Fundamentals, Devices, and Applications*, 1st ed.; Cosseddu, P.; Caironi, M., Eds.; Woodhead Publishing: Duxford, UK, 2021.

(2) Simon, D. T.; Gabrielsson, E. O.; Tybrandt, K.; Berggren, M. Organic Bioelectronics: Bridging the Signaling Gap between Biology and Technology. *Chem. Rev.* **2016**, *116*, 13009−13041.

(3) Lüssem, B.; Riede, M.; Leo, K. Doping of organic semiconductors. *Phys. Status Solidi A* **2013**, *210*, 9−43.

(4) Jacobs, I. E.; Moulé, A. J. Controlling molecular doping in organic semiconductors. *Adv. Mater.* **2017**, *29*, No. 1703063.

(5) Scaccabarozzi, A. D.; Basu, A.; Aniés, F.; Liu, J.; Zapata-Arteaga, O.; Warren, R.; Firdaus, Y.; Nugraha, M. I.; Lin, Y.; Campoy-Quiles, M.; Koch, N.; Müller, C.; Tsetseris, L.; Heeney, M.; Anthopoulos, T. D. Doping Approaches for Organic Semiconductors. *Chem. Rev.* **2022**, *122*, 4420−4492.

(6) Li, J.; Duchemin, I.; Roscioni, O. M.; Friederich, P.; Anderson, M.; Da Como, E.; Kociok-Köhn, G.; Wenzel, W.; Zannoni, C.; Beljonne, D.; Blase, X.; D'Avino, G. Host dependence of the electron affinity of molecular dopants. *Mater. Horiz.* **2019**, *6*, 107−114.

(7) Salzmann, I.; Heimel, G.; Oehzelt, M.; Winkler, S.; Koch, N. Molecular electrical doping of organic semiconductors: fundamental mechanisms and emerging dopant design rules. *Acc. Chem. Res.* **2016**, *49*, 370−378.

(8) Nell, B.; Ortstein, K.; Boltalina, O. V.; Vandewal, K. Influence of dopant−host energy level offset on thermoelectric properties of doped organic semiconductors. *J. Phys. Chem. C* **2018**, *122*, 11730−11735.

(9) Euvrard, J.; Revaux, A.; Bayle, P.-A.; Bardet, M.; Vuillaume, D.; Kahn, A. The formation of polymer-dopant aggregates as a possible origin of limited doping efficiency at high dopant concentration. *Org. Electron.* **2018**, *53*, 135−140.

(10) Duong, D. T.; Wang, C.; Antono, E.; Toney, M. F.; Salleo, A. The chemical and structural origin of efficient p-type doping in P3HT. *Org. Electron.* **2013**, *14*, 1330−1336.

(11) Dixon, A. L.; Vezin, H.; Nguyen, T.-Q.; Reddy, G. N. M. Structural insights into Lewis acid- and F4TCNQ-doped conjugated polymers by solid-state magnetic resonance spectroscopy. *Mater. Horiz.* **2022**, *9*, 981−990.

(12) Kiefer, D.; Kroon, R.; Hofmann, A. I.; Sun, H.; Liu, X.; Giovannitti, A.; Stegerer, D.; Cano, A.; Hynynen, J.; Yu, L.; Zhang, Y.; Nai, D.; Harrelson, T. F.; Sommer, M.; Moulé, A. J.; Kemerink, M.; Marder, S. R.; McCulloch, I.; Fahlman, M.; Fabiano, S.; Müller, C. Double doping of conjugated polymers with monomer molecular dopants. *Nat. Mater.* **2019**, *18*, 149−155.
(13) Goel, M.; Siegert, M.; Krauss, G.; Mohanraj, J.; Hochgesang, A.; Heinrich, D. C.; Fried, M.; Pflaum, J.; Thelakkat, M. HOMO−HOMO electron transfer: An elegant strategy for p-type doping of polymer semiconductors toward thermoelectric applications. *Adv. Mater.* **2020**, *32*, No. 2003596.
(14) Krauss, G.; Hochgesang, A.; Mohanraj, J.; Thelakkat, M. Highly Efficient Doping of Conjugated Polymers Using Multielectron Acceptor Salts. *Macromol. Rapid Commun.* **2021**, *42*, No. 2100443.
(15) Paniagua, S. A.; Baltazar, J.; Sojoudi, H.; Mohapatra, S. K.; Zhang, S.; Henderson, C. L.; Graham, S.; Barlow, S.; Marder, S. R. Production of heavily n- and p-doped CVD graphene with solution-processed redox-active metal−organic species. *Mater. Horiz.* **2014**, *1*, 111−115.
(16) Mohapatra, S. K.; Zhang, Y.; Sandhu, B.; Fonari, M. S.; Timofeeva, T. V.; Marder, S. R.; Barlow, S. Synthesis, characterization, and crystal structures of molybdenum complexes of unsymmetrical electron-poor dithiolene ligands. *Polyhedron* **2016**, *116*, 88−95.
(17) Qi, Y.; Sajoto, T.; Barlow, S.; Kim, E.-G.; Brédas, J.-L.; Marder, S. R.; Kahn, A. Use of a High Electron-Affinity Molybdenum Dithiolene Complex to p-Dope Hole-Transport Layers. *J. Am. Chem. Soc.* **2009**, *131*, 12530−12531.
(18) Hynynen, J.; Järsvall, E.; Kroon, R.; Zhang, Y.; Barlow, S.; Marder, S. R.; Kemerink, M.; Lund, A.; Müller, C. Enhanced thermoelectric power factor of tensile drawn poly(3-hexylthiophene). *ACS Macro Lett.* **2019**, *8*, 70−76.
(19) Untilova, V.; Hynynen, J.; Hofmann, A. I.; Scheunemann, D.; Zhang, Y.; Barlow, S.; Kemerink, M.; Marder, S. R.; Biniek, L.; Müller, C.; Brinkmann, M. High thermoelectric power factor of poly(3-hexylthiophene) through in-plane alignment and doping with a molybdenum dithiolene complex. *Macromolecules* **2020**, *53*, 6314−6321.
(20) Yamashita, Y.; Tsurumi, J.; Kurosawa, T.; Ueji, K.; Tsuneda, Y.; Kohno, S.; Kempe, H.; Kumagai, S.; Okamoto, T.; Takeya, J.; Watanabe, S. Supramolecular cocrystals built through redox-triggered ion intercalation in π-conjugated polymers. *Commun. Mater.* **2021**, *2*, No. 45.
(21) Jacobs, I. E.; Lin, Y.; Huang, Y.; Ren, X.; Simatos, D.; Chen, C.; Tjhe, D.; Statz, M.; Lai, L.; Finn, P. A.; Neal, W. G.; D'Avino, G.; Lemaur, V.; Fratini, S.; Beljonne, D.; Strzalka, J.; Nielsen, C. B.; Barlow, S.; Marder, S. R.; McCulloch, I.; Sirringhaus, H. High-efficiency ion-exchange doping of conducting polymers. *Adv. Mater.* **2021**, No. 2102988.
(22) Euvrard, J.; Revaux, A.; Nobre, S. S.; Kahn, A.; Vuillaume, D. Toward a better understanding of the doping mechanism involved in $Mo(tfd\text{-}COCF_3)_3$ doped PBDTTT-c. *J. Appl. Phys.* **2018**, *123*, No. 225501.
(23) Nunes Domschke, T.; Bardagot, O.; Benayad, A.; Demadrille, R.; Carella, A.; Clerc, R.; Pereira, A. Unraveling the mechanism behind air instability in thin semiconducting polymer layers p-doped with molybdenum dithiolene complexes. *Synth. Met.* **2020**, *260*, No. 116251.
(24) Barrière, F.; Camire, N.; Geiger, W. E.; Mueller-Westerhoff, U. T.; Sanders, R. Use of Medium Effects to Tune the ΔE1/2 Values of Bimetallic and Oligometallic Compounds. *J. Am. Chem. Soc.* **2002**, *124*, 7262−7263.
(25) Zokaei, S.; Kroon, R.; Gladisch, J.; Paulsen, B. D.; Sohn, W.; Hofmann, A. I.; Persson, G.; Stamm, A.; Syrén, P.-O.; Olsson, E.; Rivnay, J.; Stavrinidou, E.; Lund, A.; Müller, C. Toughening of a Soft Polar Polythiophene through Copolymerization with Hard Urethane Segments. *Adv. Sci.* **2021**, *8*, No. 2002778.
(26) Wang, E.; Hou, L.; Wang, Z.; Hellström, S.; Zhang, F.; Inganäs, O.; Andersson, M. R. An Easily Synthesized Blue Polymer for High-Performance Polymer Solar Cells. *Adv. Mater.* **2010**, *22*, 5240−5244.
(27) Kroon, R.; Gehlhaar, R.; Steckler, T. T.; Henriksson, P.; Müller, C.; Bergqvist, J.; Hadipour, A.; Heremans, P.; Andersson, M. R. New quinoxaline and pyridopyrazine-based polymers for solution-processable photovoltaics. *Sol. Energy Mater. Sol. Cells* **2012**, *105*, 280−286.
(28) Arvind, M.; Tait, C. E.; Guerrini, M.; Krumland, J.; Valencia, A. M.; Cocchi, C.; Mansour, A. E.; Koch, N.; Barlow, S.; Marder, S. R.; Behrends, J.; Neher, D. Quantitative Analysis of Doping-Induced Polarons and Charge-Transfer Complexes of Poly(3-hexylthiophene) in Solution. *J. Phys. Chem. B* **2020**, *124*, 7694−7708.
(29) Fekl, U.; Sarkar, B.; Kaim, W.; Zimmer-De Iuliis, M.; Nguyen, N. Tuning of the Spin Distribution between Ligand- and Metal-Based Spin: Electron Paramagnetic Resonance of Mixed-Ligand Molybdenum Tris(dithiolene) Complex Anions. *Inorg. Chem.* **2011**, *50*, 8685−8687.
(30) Davison, A.; Edelstein, N.; Holm, R. H.; Maki, A. H. Synthetic and Electron Spin Resonance Studies of Six-Coordinate Complexes Related by Electron-Transfer Reactions. *J. Am. Chem. Soc.* **1964**, *86*, 2799−2805.
(31) Tenderholt, A. L.; Szilagyi, R. K.; Holm, R. H.; Hodgson, K. O.; Hedman, B.; Solomon, E. I. Electronic Control of the "Bailar Twist" in Formally d0-d2 Molybdenum Tris(dithiolene) Complexes: A Sulfur K-edge X-ray Absorption Spectroscopy and Density Functional Theory Study. *Inorg. Chem.* **2008**, *47*, 6382−6392.
(32) Connelly, N. G.; Geiger, W. E. Chemical Redox Agents for Organometallic Chemistry. *Chem. Rev.* **1996**, *96*, 877−910.
(33) Hofmann, A. I.; Kroon, R.; Zokaei, S.; Järsvall, E.; Malacrida, C.; Ludwigs, S.; Biskup, T.; Müller, C. Chemical doping of conjugated polymers with the strong oxidant magic blue. *Adv. Electron. Mater.* **2020**, *6*, No. 2000249.
(34) Untilova, V.; Biskup, T.; Biniek, L.; Vijayakumar, V.; Brinkmann, M. Control of chain alignment and crystallization helps enhance charge conductivities and thermoelectric power factors in sequentially doped P3HT:F_4TCNQ films. *Macromolecules* **2020**, *53*, 2441−2453.
(35) Veregin, R. P.; Harbour, J. R. Electron spin resonance spectroscopic study of electronic charge transport in an aromatic diamine. *J. Phys. Chem. B* **1990**, *94*, 6231−6237.
(36) Kroon, R.; Kiefer, D.; Stegerer, D.; Yu, L.; Sommer, M.; Müller, C. Polar side chains enhance processability, electrical conductivity, and thermal stability of a molecularly p-doped polythiophene. *Adv. Mater.* **2017**, *29*, No. 1700930.
(37) Schröder, M.; Biskup, T. cwepr − A Python package for analysing cw-EPR data focussing on reproducibility and simple usage. *J. Magn. Reson.* **2022**, *335*, No. 107140.
(38) Schröder, M.; Biskup, T. *Cwepr Python Package*, Zenodo 2021.

https://doi.org/10.1021/acs.chemmater.2c01040
Chem. Mater. 2022, 34, 5673−5679